

On Phase Transition of $\text{NH}_4\text{H}_2\text{PO}_4$ -Type Crystals by Cluster Variation Method

Norihiro IHARA*, Shun-ichi YOSHIDA, and Koh WADA

Division of Physics, Graduate School of Science, Hokkaido University, Sapporo 060-0810

(Received November 21, 2018)

The Cluster Variation Method (CVM) is applied to the Ishibashi model for ammonium dihydrogen phosphate ($\text{NH}_4\text{H}_2\text{PO}_4$) of a typical hydrogen bonded anti-ferroelectric crystal. The staggered and the uniform susceptibility without hysteresis are calculated at equilibrium. On the other hand, by making use of the natural iteration method (NIM) for the CVM, hysteresis phenomena of uniform susceptibility versus temperature observed in experiments is well explained on the basis of local minimum in Landau type variational free energy. The polarization P curves against the uniform field is also calculated.

KEYWORDS: $\text{NH}_4\text{H}_2\text{PO}_4$ (ADP), anti-ferroelectrics, Ishibashi model, Cluster Variation Method (CVM), Natural Iteration Method (NIM), susceptibility

* E-mail: ihara@statphys.sci.hokudai.ac.jp

§1. Introduction

Recently, the pyrochlore oxide crystals $A_2B_2O_7$ ($A=Ho, Dy, B=Sn, Ti$) called the spin ice have drawn many attentions of researchers.¹⁾ The spin ice system has a typical geometrical frustration structure. The similar frustration structure is found in ammonium dihydrogen phosphate $NH_4H_2PO_4$ (ADP). ADP is one of the hydrogen bonded crystals similar to well-known potassium dihydrogen phosphate KH_2PO_4 (KDP). However, as a result of the replacement of potassium ion K^+ by ammonium ion NH_4^+ , ADP undergoes the anti-ferroelectric phase transition while KDP is the typical ferroelectrics. Nagamiya²⁾ first suggested a possibility of anti-ferroelectricity for ADP in the framework of the Slater's model for KDP³⁾ in which the replacement of the first excited energy ε_0 due to hydrogen configuration around PO_4 by a negative value $-\varepsilon_0$ might well explain the experimental behaviors in ADP. However, Ishibashi *et al.*⁴⁾ pointed out that only taking negative value $-\varepsilon_0$ is not enough to realize the antiferroelectric phase transition because there are several proton configurations with the same energy as that proposed by Nagamiya due to geometrical frustration. In order to single out the observed crystal structure in ADP experiments, Ishibashi introduced the dipole-dipole interaction in Nagamiya's proposed model. Ishibashi⁵⁾ further analyzed the extended model (hereafter Ishibashi model) in which it is possible for three or four protons to come closer to a PO_4 tetrahedron contrary to the ice rule. Here the ice rule demands: (1) each bond connecting the oxygen atoms in neighboring PO_4 tetrahedra has always one and only one proton, and (2) each PO_4 tetrahedron can have only two protons near-by. Namely the second rule of the ice rule is loosened in the Ishibashi model. The model with this type of extension for the Slater's KDP theory is often called the Slater-Takagi model.⁶⁾

In the present paper the Ishibashi model for ADP is reconsidered for the preliminary study of pyrochlore crystals with geometrical frustration structure. We calculate the staggered and the uniform susceptibility above and below the transition temperature in the Ishibashi model for the ADP-type crystal in the cactus approximation of the cluster variation method⁷⁾ which is equivalent to the Slater's approximation for the KDP model. Further, the hysteresis phenomena of uniform susceptibility versus temperature observed in experiments are successfully shown by making use of the natural iteration method (NIM) developed by Kikuchi.⁸⁾ As the case of hysteresis phenomena depending upon the external electric field, the polarization P curves against the uniform field is also calculated.

In §2 we derive the variational free energy in the cactus approximation of the CVM.⁹⁾ In §3, from thermal equilibrium condition we obtain a self-consistent equation for polarization in a staggered electric field in order to find the properties of phase transition in the present system. After determining the tricritical point which stands for the boundary between the first and the second order phase transition, we calculate the staggered susceptibility and the antiferroelectric sublattice spontaneous polarization. In §4, after we calculate the uniform susceptibility of the present system in

thermal equilibrium, we study hysteresis phenomena of uniform susceptibility versus temperature in order to compare with the experimental results. §5 is devoted to a summary.

§2. Formulation

Let us consider the system consisting of $2N$ protons around N PO_4 tetrahedra in the ADP-type crystal as shown in Fig. 1. In order to formulate the present system in which the anti-ferroelectric phase transition along the a -axis takes place, we take a four sublattice model by Ishibashi⁵⁾ as shown in Fig. 2. Here p, q, r and s denote non-equivalent hydrogen bonds on which a proton is located. When a proton on the hydrogen bond p is located close to the i -th sublattice, we denote the occurrence probability of such a proton configuration as p_i . Next, let us assign the energy, the occurrence probability and the dipole moment along the a -axis to the protons configuration around PO_4 tetrahedron as shown in Fig. 3. We apply the cactus approximation of the CVM to the present system so as to find the variational free energy. The cactus approximation of the CVM is equivalent to the Slater's theory for KDP which takes account of the site of a proton in the double well potential along each O-O bond (hydrogen bond) between two nearest neighbor PO_4 tetrahedra and the correlation of four protons around each PO_4 tetrahedron. In the following we call the occurrence probability of a proton configuration on the hydrogen bond as a bond (state) variable and that of four protons configuration around PO_4 tetrahedron as a four protons (state) variable. The number of configurations of L ensemble in the cactus approximation of the CVM is given by⁷⁾

$$W = \prod_{i=1}^{2N} W_{\text{bond}}^{(i)} \prod_{\langle ijkl \rangle} G_{\text{tetra}}^{(ijkl)}, \quad (2.1)$$

with

$$G_{\text{tetra}}^{(ijkl)} = \frac{W_{\text{tetra}}^{(ijkl)}}{W_{\text{bond}}^{(i)} W_{\text{bond}}^{(j)} W_{\text{bond}}^{(k)} W_{\text{bond}}^{(l)}}, \quad (2.2)$$

where, for example, $W_{\text{bond}}^{(i)}$ is the number of proton configurations on the i -th bond if the i -th bond is p bond between 1 and 2 sublattice:

$$W_{\text{bond}}^{(i)} = \frac{L!}{(Lp_1)!(Lp_2)!}, \quad (2.3)$$

and $G_{\text{tetra}}^{(ijkl)}$ is the correlation number of protons for a PO_4 tetrahedron surrounded by protons on the i, j, k, l hydrogen bonds. And $W_{\text{tetra}}^{(ijkl)}$ is the number of four protons configuration around PO_4 surrounded by protons on the i, j, k, l bonds. For example, referring to Fig. 3, for a PO_4 tetrahedron belonging to the 1-st sublattice, $W_{\text{tetra}}^{(ijkl)}$ is given by

$$W_{\text{tetra}}^{(ijkl)} = \frac{L!}{[(Lc_0^{(1)})!]^2 [(Lc_2^{(1)})!]^2 (La_+^{(1)})! (La_-^{(1)})! [(La_0^{(1)})!]^2 [(Ld_+^{(1)})!]^4 [(Ld_-^{(1)})!]^4}, \quad (2.4)$$

where the superscript (1) denotes the number of sublattice. By utilizing Stirling's formula and assuming the homogeneity in each sublattice, the entropy of the present four sublattice model becomes

$$\begin{aligned}
\frac{S}{k_B} &= \frac{1}{L} \log W \\
&= \frac{N}{4} \sum_{i=1}^4 \left[p_i \ln p_i + q_i \ln q_i + r_i \ln r_i + s_i \ln s_i \right. \\
&\quad - \left(a_+^{(i)} \ln a_+^{(i)} + a_-^{(i)} \ln a_-^{(i)} + 4d_+^{(i)} \ln d_+^{(i)} \right. \\
&\quad \left. + 4d_-^{(i)} \ln d_-^{(i)} + 2a_0^{(i)} \ln a_0^{(i)} \right. \\
&\quad \left. + 2c_0^{(i)} \ln c_0^{(i)} + 2c_2^{(i)} \ln c_2^{(i)} \right). \tag{2.5}
\end{aligned}$$

Further, the electric polarization of i -th sublattice per PO_4 along the a -axis is defined by

$$\mu_a P^{(i)} = \mu_a [(a_+^{(i)} - a_-^{(i)}) + 2(d_+^{(i)} - d_-^{(i)})] \quad (i = 1 \sim 4), \tag{2.6}$$

where μ_a is the dipole moment along the a -axis. The proton configuration energy U per system is given by

$$\begin{aligned}
U &= \frac{N}{4} \sum_{i=1}^4 [2\varepsilon_0 c_0^{(i)} + 4\varepsilon_1 (d_+^{(i)} + d_-^{(i)}) + 2\varepsilon_2 c_2^{(i)}] \\
&\quad + \frac{N}{4} \lambda \mu_a^2 (P^{(1)} + P^{(2)})(P^{(3)} + P^{(4)}) \\
&\quad - \frac{N}{4} [\mu_a E (P^{(1)} + P^{(2)}) + \mu_a E' (P^{(3)} + P^{(4)})], \tag{2.7}
\end{aligned}$$

where the first line represents the protons configuration energy around PO_4 tetrahedra, the second line denotes effectively the long range dipole-dipole interaction energy to induce an anti-ferroelectric structure along the a -axis and the last line is the energy due to external electric field. In the following we call the case of $E' = -E$ a staggered electric field and the case of $E' = E$ a homogeneous electric field. Here it should be noted that bond variables are always expressed in terms of four protons variables:

$$\begin{aligned}
2p_1 = 2q_2 &= c_0^{(1)} + c_2^{(1)} + a_0^{(1)} + a_+^{(1)} + 3d_+^{(1)} + d_-^{(1)} \\
&\quad + c_0^{(2)} + c_2^{(2)} + a_0^{(2)} + a_+^{(2)} + 3d_+^{(2)} + d_-^{(2)}, \\
2p_2 = 2q_1 &= c_0^{(1)} + c_2^{(1)} + a_0^{(1)} + a_-^{(1)} + d_+^{(1)} + 3d_-^{(1)} \\
&\quad + c_0^{(2)} + c_2^{(2)} + a_0^{(2)} + a_-^{(2)} + d_+^{(2)} + 3d_-^{(2)}, \\
2r_1 = 2s_3 &= c_0^{(1)} + c_2^{(1)} + a_0^{(1)} + a_+^{(1)} + 3d_+^{(1)} + d_-^{(1)} \\
&\quad + c_0^{(3)} + c_2^{(3)} + a_0^{(3)} + a_-^{(3)} + d_+^{(3)} + 3d_-^{(3)}, \\
2r_3 = 2s_1 &= c_0^{(1)} + c_2^{(1)} + a_0^{(1)} + a_-^{(1)} + d_+^{(1)} + 3d_-^{(1)}
\end{aligned}$$

$$\begin{aligned}
& +c_0^{(3)} + c_2^{(3)} + a_0^{(3)} + a_+^{(3)} + 3d_+^{(3)} + d_-^{(3)}, \\
2p_3 = 2q_4 = & c_0^{(3)} + c_2^{(3)} + a_0^{(3)} + a_-^{(3)} + d_+^{(3)} + 3d_-^{(3)} \\
& +c_0^{(4)} + c_2^{(4)} + a_0^{(4)} + a_-^{(4)} + d_+^{(4)} + 3d_-^{(4)}, \\
2p_4 = 2q_3 = & c_0^{(3)} + c_2^{(3)} + a_0^{(3)} + a_+^{(3)} + 3d_+^{(3)} + d_-^{(3)} \\
& +c_0^{(4)} + c_2^{(4)} + a_0^{(4)} + a_+^{(4)} + 3d_+^{(4)} + d_-^{(4)}, \\
2r_2 = 2s_4 = & c_0^{(2)} + c_2^{(2)} + a_0^{(2)} + a_+^{(2)} + 3d_+^{(2)} + d_-^{(2)} \\
& +c_0^{(4)} + c_2^{(4)} + a_0^{(4)} + a_-^{(4)} + d_+^{(4)} + 3d_-^{(4)}, \\
2r_4 = 2s_2 = & c_0^{(2)} + c_2^{(2)} + a_0^{(2)} + a_-^{(2)} + d_+^{(2)} + 3d_-^{(2)} \\
& +c_0^{(4)} + c_2^{(4)} + a_0^{(4)} + a_+^{(4)} + 3d_+^{(4)} + d_-^{(4)}.
\end{aligned} \tag{2.8}$$

There are also normalization relations among four protons state variables:

$$\begin{aligned}
a_+^{(i)} + a_-^{(i)} + 4(d_+^{(i)} + d_-^{(i)}) + 2a_0^{(i)} + 2c_0^{(i)} + 2c_2^{(i)} = 1 \\
(i = 1 \sim 4),
\end{aligned} \tag{2.9}$$

where the superscript (i) denotes the sublattice number. Finally, by combining eq.(2.5) and eq.(2.7) the variational free energy G in the cactus approximation is obtained by

$$G = U - TS. \tag{2.10}$$

§3. Response to Staggered Electric Field

Let us calculate the staggered susceptibility to study the properties of phase transition of the system. The staggered field is applied so as to induce the anti-ferroelectric order. Since the anti-ferroelectric structure is assumed to occur along the a -axis, the electric field $E' = -E$ is applied to the sublattice 3 and 4 in addition of E to the sublattice 1 and 2. Since the sublattice 3 and 4 are equivalent to 1 and 2 except having a sublattice polarization in the opposite direction, the present system is reduced to the one sublattice problem and we have following relations

$$\begin{aligned}
a_0^{(i)} = a_0, \quad c_0^{(i)} = c_0, \quad c_2^{(i)} = c_2 \quad (i = 1 \sim 4), \\
a_{\pm}^{(1)} = a_{\pm}^{(2)} = a_{\mp}^{(3)} = a_{\mp}^{(4)} = a_{\pm}, \\
d_{\pm}^{(1)} = d_{\pm}^{(2)} = d_{\mp}^{(3)} = d_{\mp}^{(4)} = d_{\pm}, \\
p_1 = p_3 = q_2 = q_4 = r_1 = r_2 = s_3 = s_4 \\
= c_0 + c_2 + a_0 + a_+ + 3d_+ + d_-, \\
p_2 = p_4 = q_1 = q_3 = r_3 = r_4 = s_1 = s_2 \\
= c_0 + c_2 + a_0 + a_- + d_+ + 3d_-.
\end{aligned} \tag{3.1}$$

And the sublattice polarization conjugate to the staggered field is now given by

$$\begin{aligned} P &\equiv P^{(1)} = P^{(2)} = -P^{(3)} = -P^{(4)} \\ &= a_+ - a_- + 2(d_+ - d_-) = p_1 - p_2. \end{aligned} \quad (3.2)$$

The free energy G of the system takes a form:

$$\begin{aligned} \frac{G}{Nk_B T} &= \left[\frac{2\varepsilon_0}{k_B T} c_0 + \frac{4\varepsilon_1}{k_B T} (d_+ + d_-) + \frac{2\varepsilon_2}{k_B T} c_2 \right] - \frac{\lambda \mu_a^2}{k_B T} P^2 \\ &\quad - \frac{\mu_a E P}{k_B T} + \left[-2 \left(\frac{1+P}{2} \ln \frac{1+P}{2} + \frac{1-P}{2} \ln \frac{1-P}{2} \right) \right. \\ &\quad \left. + (a_+ \ln a_+ + a_- \ln a_- + 2a_0 \ln a_0 \right. \\ &\quad \left. + 2c_0 \ln c_0 + 2c_2 \ln c_2 + 4d_+ \ln d_+ + 4d_- \ln d_-) \right] \\ &\quad + \frac{\gamma}{k_B T} [1 - (a_+ + a_- + 4(d_+ + d_-) + 2a_0 + 2c_0 + 2c_2)], \end{aligned} \quad (3.3)$$

where γ in the last line is the Lagrange multiplier to make all the state variables $a_+, a_-, a_0, d_+, d_-, c_0, c_2$ independent. Under the staggered electric field the thermal equilibrium state is obtained from the minimum condition of the free energy: $\frac{\partial G}{\partial a_+} = \frac{\partial G}{\partial a_-} = \frac{\partial G}{\partial d_+} = \frac{\partial G}{\partial d_-} = \frac{\partial G}{\partial a_0} = \frac{\partial G}{\partial c_0} = \frac{\partial G}{\partial c_2} = 0$. The state variables are solved in terms of a_0 , the electric polarization P and the staggered field E as follows:

$$\begin{aligned} c_0 &= \eta_0 a_0, & c_2 &= \eta_2 a_0, \\ a_+ &= a_0 A_P h^2, & a_- &= a_0 (A_P h^2)^{-1}, \\ d_+ &= a_0 \eta_1 A_P^{\frac{1}{2}} h, & d_- &= a_0 \eta_1 A_P^{-\frac{1}{2}} h^{-1}, \end{aligned} \quad (3.4)$$

where $\eta_0 = \exp(-\varepsilon_0/k_B T)$, $\eta_1 = \exp(-\varepsilon_1/k_B T)$, $\eta_2 = \exp(-\varepsilon_2/k_B T)$, $h = \exp \frac{\mu_a E}{2k_B T}$ and an abbreviation is defined as

$$A_P = \frac{1+P}{1-P} \exp(2DP) \quad (D \equiv \frac{\lambda \mu_a^2}{k_B T}). \quad (3.5)$$

Further, a_0 is determined by a normalization condition as

$$\begin{aligned} a_0 &= \left[2 + 2\eta_0 + 2\eta_2 + A_P h^2 + A_P^{-1} h^{-2} \right. \\ &\quad \left. + 4\eta_1 (A_P^{\frac{1}{2}} h + A_P^{-\frac{1}{2}} h^{-1}) \right]^{-1}. \end{aligned} \quad (3.6)$$

Substituting eq.(3.4) and eq.(3.6) into the variational free energy of eq.(3.3), the equilibrium free energy G_e under the staggered field is given by

$$\frac{G_e}{Nk_B T} = \ln \frac{4a_0}{(1-P^2)} + \frac{\lambda}{k_B T} P^2. \quad (3.7)$$

Without staggered field this expression has been obtained by Ishibashi.⁵⁾ The sublattice polarization P under the staggered field is obtained as a self-consistent equation from eq.(3.2):

$$P = a_0 \left[A_P h^2 - A_P^{-1} h^{-2} + 2\eta_1 (A_P^{\frac{1}{2}} h - A_P^{-\frac{1}{2}} h^{-1}) \right]. \quad (3.8)$$

The same self-consistent equation for P is also obtained by the thermodynamic relation $N\mu_a P = -\frac{1}{k_B T} \frac{\partial G}{\partial E}$.

In order to investigate the phase transition properties we expand the above equation (3.8) up to the 3-rd order of polarization P and to the linear order of staggered field E in the neighborhood of the transition temperature:

$$A_2(T)P + A_4(T)P^3 + \dots - 4(1 + \eta_1)\frac{\mu_a E}{k_B T} = 0, \quad (3.9)$$

where $A_2(T)$ and $A_4(T)$ are given by

$$\begin{aligned} A_2(T) &= 2\eta_0 + 4\eta_1 + 2\eta_2 - 4(1 + \eta_1)D, \\ A_4(T) &= -4D^2 - \frac{8D^3}{3} + 2\eta_1(1 + 3D + D^2 - \frac{D^3}{3}). \end{aligned} \quad (3.10)$$

From the view point of Landau's phase transition theory the order of the phase transition is classified as follows. (i) The phase transition undergoes the second order transition at T_0 if $A_2(T_0) = 0$ and $A_4(T_0) > 0$. (ii) The phase transition undergoes the first order transition at $T_C (> T_0)$ if $A_2(T_0) = 0$ and $A_4(T_0) < 0$. The boundary between the first and the second order transition is called the tricritical point $T_t (= T_0)$ when $A_2(T_0) = 0$ and $A_4(T_0) = 0$. The phase diagram in the $\varepsilon_1 - T$ space is shown in Fig. 4. Hereafter the parameters $\varepsilon_0 = 6k_B, \varepsilon_2 = 1000k_B, \lambda = 232k_B$ are taken. It can be seen that the energy parameter ε_1 representing HPO_4 and H_3PO_4 controls the order of phase transition. As $\varepsilon_1/\varepsilon_0$ is increased, the second order phase transition for small $\varepsilon_1/\varepsilon_0$ changes into the first order transition. In any case the spontaneous sublattice polarization P_0 of the anti-ferroelectric state is given by the self-consistent equation (3.8) without electric field:

$$P_0 = \hat{a}_0 [A_{P_0} - A_{P_0}^{-1} + 2\eta_1 (A_{P_0}^{\frac{1}{2}} - A_{P_0}^{-\frac{1}{2}})], \quad (3.11)$$

where \hat{a}_0 is a thermal equilibrium value of a_0 in eq.(3.6) without external field. We solve eq.(3.11) numerically and show the spontaneous polarization P_0 versus temperature in Fig. 5. On the other side, the staggered susceptibility χ_s of the system is obtained from eq.(3.8) as the linear response ΔP from P_0 induced by the staggered field E

$$\chi_s(T) = \lim_{E \rightarrow 0} N\mu_a \frac{\Delta P}{E} = \frac{N\mu_a^2}{k_B T} \frac{1}{X^{-1} - (\frac{1}{1-P_0^2} + D)} \quad (3.12)$$

with

$$X = 2\hat{a}_0 \left[A_{P_0} + A_{P_0}^{-1} + \eta_1 (A_{P_0}^{\frac{1}{2}} + A_{P_0}^{-\frac{1}{2}}) \right] - 2P_0^2.$$

Especially, in the paraelectric phase the staggered susceptibility is simplified into

$$\chi_s(T) = \frac{N\mu_a^2}{k_B T} \frac{2(1 + \eta_1)}{\eta_0 + 2\eta_1 + \eta_2 - 2(1 + \eta_1)D}. \quad (3.13)$$

The staggered susceptibility $\chi_s(T)$ is shown in Fig. 6 for each case of the second and the first order transition. It is noteworthy that when we choose $D = 0$, the staggered susceptibility never diverges. Without a finite dipole-dipole interaction parameter λ , we would have the paraelectric state down to the zero temperature owing to geometrical frustration structure of the system.

§4. Response to Uniform Electric Field

Let us study the response of the present system to a uniform electric field along the a -axis. The same external electric field $E' = E$ is applied to the sublattice 3 and 4 as well as to the sublattice 1 and 2. Contrary to the case of staggered electric field, in the anti-ferroelectric state the sublattice 1 and 2 are non-equivalent to the sublattice 3 and 4 in response to the uniform electric field. The present system is reduced to the two sublattice problem and we have following relations:

$$\begin{aligned} a_0^{(i)} &= a_0, & c_0^{(i)} &= c_0, & c_2^{(i)} &= c_2 & (i = 1 \sim 4), \\ a_{\pm}^{(1)} &= a_{\pm}^{(2)} = a_{\pm}, & a_{\pm}^{(3)} &= a_{\pm}^{(4)} = a'_{\mp}, \\ d_{\pm}^{(1)} &= d_{\pm}^{(2)} = d_{\pm}, & d_{\pm}^{(3)} &= d_{\pm}^{(4)} = d'_{\mp}, \\ p_1 &= q_2 = c_0 + c_2 + a_0 + a_+ + 3d_+ + d_-, \\ p_2 &= q_1 = c_0 + c_2 + a_0 + a_- + d_+ + 3d_-, \\ p_3 &= q_4 = c_0 + c_2 + a_0 + a'_+ + 3d'_+ + d'_-, \\ p_4 &= q_3 = c_0 + c_2 + a_0 + a'_- + d'_+ + 3d'_-, \\ 2r_1 &= 2s_3 = 2r_2 = 2s_4 \\ &= 2c_0 + 2c_2 + 2a_0 + a_+ + a'_+ + 3(d_+ + d'_+) + (d_- + d'_-), \\ 2r_3 &= 2s_1 = 2r_4 = 2s_2 \\ &= 2c_0 + 2c_2 + 2a_0 + a_- + a'_- + (d_+ + d'_+) + 3(d_- + d'_-). \end{aligned} \quad (4.1)$$

And the sublattice electric polarizations along the a -axis are defined as

$$\begin{aligned} P &\equiv P^{(1)} = P^{(2)} = a_+ - a_- + 2(d_+ - d_-) = p_1 - p_2, \\ P' &\equiv -P^{(3)} = -P^{(4)} = a'_+ - a'_- + 2(d'_+ - d'_-) = p_3 - p_4. \end{aligned} \quad (4.2)$$

The variational free energy G in the uniform field is rewritten as

$$\begin{aligned} \frac{G}{Nk_B T} &= 2 \left[\frac{\varepsilon_0 c_0}{k_B T} + \frac{\varepsilon_1}{k_B T} (d_+ + d_- + d'_+ + d'_-) + \frac{\varepsilon_2 c_2}{k_B T} \right] \\ &\quad - \frac{\lambda \mu_a^2}{k_B T} P P' - \frac{\mu_a E}{2k_B T} (P - P') \end{aligned}$$

$$\begin{aligned}
& -\frac{1}{2}[(p_1 \ln p_1 + p_2 \ln p_2) + 2(r_1 \ln r_1 + r_3 \ln r_3)] \\
& + (p_3 \ln p_3 + p_4 \ln p_4) \\
& + \frac{1}{2}[a_+ \ln a_+ + a_- \ln a_- + a'_+ \ln a'_+ + a'_- \ln a'_- \\
& + 4a_0 \ln a_0 + 4c_0 \ln c_0 + 4c_2 \ln c_2 \\
& + 4(d_+ \ln d_+ + d_- \ln d_-) + 4(d'_+ \ln d'_+ + d'_- \ln d'_-)] \\
& + \frac{\gamma_1}{k_B T} [1 - (a_+ + a_- + 4(d_+ + d_-) + 2a_0 + 2c_0 + 2c_2)] \\
& + \frac{\gamma_2}{k_B T} [1 - (a'_+ + a'_- + 4(d'_+ + d'_-) + 2a_0 + 2c_0 + 2c_2)],
\end{aligned} \tag{4.3}$$

where γ_1 and γ_2 are Lagrange multipliers which are determined by the normalization relations (2.9) with the help of eq.(4.1). The thermal equilibrium is determined by the minimum condition of the free energy with respect to independent variables: $\frac{\partial G}{\partial a_+} = \frac{\partial G}{\partial a_-} = \frac{\partial G}{\partial d_+} = \frac{\partial G}{\partial d_-} = \frac{\partial G}{\partial a'_+} = \frac{\partial G}{\partial a'_-} = \frac{\partial G}{\partial d'_+} = \frac{\partial G}{\partial d'_-} = \frac{\partial G}{\partial a_0} = \frac{\partial G}{\partial c_0} = \frac{\partial G}{\partial c_2} = 0$. These relations are regarded as a set of equations of state in the present system under a homogeneous electric field. In Appendix A it is shown that all the independent variables are expressed in terms of sublattice polarizations P and P' under the external electric field E . Since the linear response of sublattice polarization to the uniform field E is written as $\Delta P = P - P_0$ for the 1 and 2 sublattices and $\Delta P' = P' - P'_0$ for the 3 and 4 sublattices, the uniform susceptibility χ_h is defined as

$$\chi_h = \lim_{E \rightarrow 0} \frac{N}{2} \mu_a^2 \frac{\Delta P - \Delta P'}{E}. \tag{4.4}$$

Since concrete calculations are complicated and tedious, details of the calculation and the final result are given in Appendix A. Here we mention only the homogeneous susceptibility of the system in the para-electric phase

$$\chi_h = \frac{N \mu_a^2}{k_B T} \frac{4 + 4\eta_1}{1 + \eta_0 + 3\eta_1 + \eta_2 + \frac{D}{2}(1 + \eta_1)}. \tag{4.5}$$

The numerical results of the uniform susceptibility χ_h against temperature are shown in Fig. 7 for each case of the second order and the first order transition.

However, the present uniform susceptibility in the first order transition is completely different from experimentally observed one.¹⁰⁾ The observed susceptibility shows the hysteresis phenomena versus temperature. Until now, we have obtained the susceptibility versus temperature by determining the global minimum of the variational free energy at thermal equilibrium for each temperature. However, since the heating and cooling process are done at the rate of finite time in the experiment, we cannot observe the susceptibility at thermal equilibrium. In order to solve this discrepancy, we apply the iteration method called the NIM (natural iteration method)⁸⁾ for numerical calculations of the CVM. The present iteration method leads us to the local minimum of

the variational free energy depending upon the initial condition. It should be noted that the local minimum is not always the global minimum of the free energy at each temperature. With use of the local minimum under the previous temperature as a starting point the sweeping of temperature continuously gives the hysteresis curve in the heating and the cooling process (Fig. 8). In order to explain the hysteresis phenomena versus temperature we show the temperature change in the variational free energy in Fig. 9. Let two temperatures at which a drastic change of uniform susceptibility occurs in Fig. 8 be defined as T_1 and T_2 ($T_1 < T_c < T_2$). In the heating process, (1) when $T < T_1$, A in Fig. 8 exists in a local minimum denoted by A_0 in Fig. 9, (2) when $T_1 < T < T_2$, B in Fig. 8 exists still in A_0 though another local minimum denoted by B_0 appears in Fig. 9, (3) at $T = T_c$ the three local minima have the same value and (4) at $T = T_2$, B in Fig. 8 jumps up to D in Fig. 8 because the state at the unstable A_0 in Fig. 9 tumbles into the stable B_0 . In the cooling process from D the similar free energy change occurs as a reversible process of the above. The actual usage of the NIM is explained more in detail in Appendix B.

We also calculate the hysteresis curve for the net polarization $\Delta P = (P - P')/2$ versus homogeneous electric field. The numerical result of $\Delta P - E$ curve is shown in Fig. 10. We can see clearly the transition from the anti-ferroelectric state to the polar state at which each polarization in two sublattices points to the same direction at $E = E_1$ or $E = -E_1$.

§5. A Summary and Discussions

We applied the cactus approximation of the CVM to the Ishibashi model for the hydrogen bonded ADP-type crystal. The properties of the ADP-type crystal in external electric fields were intensively investigated. After re-deriving the variational free energy for the Ishibashi model, the equation determining the polarization and the susceptibility in a staggered electric field were studied to find the order of the transition. The energy parameter ε_1 characteristic of HPO_4 and H_3PO_4 determines the properties of transition, though ADP undergoes the first order paraelectric-antiferroelectric phase transition in experiments. We also calculated the susceptibility to a homogeneous electric field at thermal equilibrium. The calculated susceptibility does not show any hysteresis even in the parameter region of the first order transition, while the homogeneous susceptibility observed in experiments shows the hysteresis phenomena in the heating and the cooling process. In order to overcome this discrepancy the homogeneous susceptibility in the local minimum of free energy was calculated and the result is in qualitatively good agreement with the experiments. The hysteresis curve is well explained by utilizing the local minimum in the variational free energy. Further, though the typical hysteresis curve of the net polarization versus homogeneous electric field have not been found in the ADP experiments to our scarce knowledge, we also calculated the hysteresis curve depending upon the external electric field with the same idea. The results are the ones expected from the Landau theory of the phase transition in the external field.

Though in the Ishibashi model the dipole-dipole interaction is included to induce an anti-

ferroelectric transition, the present model without dipole-dipole interaction has essentially the geometrical frustration and is similar to the spin ice system with ice rule. We will discuss the spin ice system from the same view point of the cluster variation method (CVM) in the near future.

The calculation of the dynamical susceptibility for the ADP-type crystal by the dynamical cluster variation method¹¹⁾ is also in progress in order to compare with the experimental data and that¹²⁾ for KDP.

Acknowledgments

We would like to thank Prof. M. Tokunaga and also our laboratory members of statistical physics for discussions and encouragements.

Appendix A: Calculation of Uniform Susceptibility

From the minimum conditions for the free energy G in eq.(4.3)

$\frac{\partial G}{\partial a_+} = \frac{\partial G}{\partial a_-} = \frac{\partial G}{\partial d_+} = \frac{\partial G}{\partial d_-} = \frac{\partial G}{\partial a'_+} = \frac{\partial G}{\partial a'_-} = \frac{\partial G}{\partial d'_+} = \frac{\partial G}{\partial d'_-} = \frac{\partial G}{\partial a_0} = \frac{\partial G}{\partial c_0} = \frac{\partial G}{\partial c_2} = 0$, the following equations are obtained:

$$\begin{aligned}
a_0 &= \frac{1}{(2 + 2\eta_0 + 2\eta_2) + tR_1R_2}, \\
c_0 &= \eta_0 a_0, \\
c_2 &= \eta_2 a_0, \\
a_+ &= \frac{R_1}{R_2} t a_0 \left(p_1 r_1 e^{2D(p_3-p_4)} \right) h^2, \\
a_- &= \frac{R_1}{R_2} t a_0 \left(p_2 r_3 e^{-2D(p_3-p_4)} \right) h^{-2}, \\
d_+ &= \frac{R_1}{R_2} t a_0 \eta_1 \left(p_1^3 p_2 r_1^3 r_3 \right)^{\frac{1}{4}} e^{D(p_3-p_4)} h, \\
d_- &= \frac{R_1}{R_2} t a_0 \eta_1 \left(p_1 p_2^3 r_1 r_3^3 \right)^{\frac{1}{4}} e^{-D(p_3-p_4)} h^{-1}, \\
a'_+ &= \frac{R_2}{R_1} t a_0 \left(p_3 r_1 e^{2D(p_1-p_2)} \right) h^{-2}, \\
a'_- &= \frac{R_2}{R_1} t a_0 \left(p_4 r_3 e^{-2D(p_1-p_2)} \right) h^2, \\
d'_+ &= \frac{R_2}{R_1} t a_0 \eta_1 \left(p_3^3 p_4 r_1^3 r_3 \right)^{\frac{1}{4}} e^{D(p_1-p_2)} h^{-1}, \\
d'_- &= \frac{R_2}{R_1} t a_0 \eta_1 \left(p_3 p_4^3 r_1 r_3^3 \right)^{\frac{1}{4}} e^{-D(p_1-p_2)} h,
\end{aligned} \tag{A.1}$$

where t , R_1 and R_2 are defined by

$$\begin{aligned}
t &= \frac{1}{[p_1 p_2 p_3 p_4 (r_1 r_3)^2]^{\frac{1}{4}}}, \\
R_1 &= [p_3 r_1 e^{2D(p_1-p_2)} h^{-2} + p_4 r_3 e^{-2D(p_1-p_2)} h^2 \\
&\quad + 4\eta_1 \left(p_3^3 p_4 r_1^3 r_3 \right)^{\frac{1}{4}} e^{D(p_1-p_2)} h^{-1}
\end{aligned}$$

$$+ \left(p_3 p_4^3 r_1 r_3^3 \right)^{\frac{1}{4}} e^{-D(p_1-p_2)h}]^{\frac{1}{2}}, \quad (\text{A}\cdot 2)$$

A set of self-consistent equation for sublattice polarizations P and P' are obtained from

$$\begin{aligned} P &= p_1 - p_2 = a_+ - a_- + 2(d_+ - d_-), \\ P' &= p_3 - p_4 = a'_+ - a'_- + 2(d'_+ - d'_-). \end{aligned} \quad (\text{A}\cdot 3)$$

Substitutions of above relations into eq.(A·3) lead us to

$$\begin{aligned} P &= \frac{R_1}{R_2} a_0 t \left\{ p_1 r_1 e^{2D(p_3-p_4)h^2} - p_2 r_3 e^{-2D(p_3-p_4)h^{-2}} \right. \\ &\quad + 2\eta_1 \left[\left(p_1^3 p_2 r_1^3 r_3 \right)^{\frac{1}{4}} e^{D(p_3-p_4)h} \right. \\ &\quad \left. \left. - \left(p_1 p_2^3 r_1 r_3^3 \right)^{\frac{1}{4}} e^{-D(p_3-p_4)h^{-1}} \right] \right\}, \\ P' &= \frac{R_2}{R_1} a_0 t \left\{ p_3 r_1 e^{2D(p_1-p_2)h^{-2}} - p_4 r_3 e^{-2D(p_1-p_2)h^2} \right. \\ &\quad + 2\eta_1 \left[\left(p_3^3 p_4 r_1^3 r_3 \right)^{\frac{1}{4}} e^{D(p_1-p_2)h^{-1}} \right. \\ &\quad \left. \left. - \left(p_3 p_4^3 r_1 r_3^3 \right)^{\frac{1}{4}} e^{-D(p_1-p_2)h} \right] \right\}, \end{aligned} \quad (\text{A}\cdot 4)$$

where it should be noted that $p_1, p_2, p_3, p_4, r_1, r_3$ are expressed in the sublattice polarization P and P' :

$$\begin{aligned} p_1 &= \frac{1}{2}(1 + P), & p_2 &= \frac{1}{2}(1 - P), \\ p_3 &= \frac{1}{2}(1 + P'), & p_4 &= \frac{1}{2}(1 - P'), \\ r_1 &= \frac{1}{2}\left(1 + \frac{P + P'}{2}\right), & r_3 &= \frac{1}{2}\left(1 - \frac{P + P'}{2}\right). \end{aligned} \quad (\text{A}\cdot 5)$$

Thus, eq.(A·4) is the self-consistent equation for P and P' . Since the linear response of sublattice polarization to the uniform external field E is defined as $\Delta P = P - P_0$ and $\Delta P' = P' - P_0$, the uniform susceptibility χ_h is obtained from eq.(A·4) as

$$\chi_h = \lim_{E \rightarrow 0} \frac{N}{2} \mu_a^2 \frac{\Delta P - \Delta P'}{E} = \frac{N \mu_a^2 Q_1}{k_B T Q_2}, \quad (\text{A}\cdot 6)$$

where

$$\begin{aligned} Q_1 &= 4 \left[A_{P_0} + A_{P_0}^{-1} + \eta_1 (A_{P_0}^{\frac{1}{2}} + A_{P_0}^{-\frac{1}{2}}) \right] \\ &\quad - \frac{4P_0^2}{\hat{a}_0^2 [A_{P_0} + A_{P_0}^{-1} + 4\eta_1 (A_{P_0}^{\frac{1}{2}} + A_{P_0}^{-\frac{1}{2}})]}, \end{aligned}$$

Appendix B: Natural Iteration Method

The natural iteration method (NIM)⁸⁾ is one of the method for determining state variables from the minimum condition of the variational free energy. Here the NIM is briefly explained from starting with eq.(A.1). It should be noted that bond variables are characteristic of one proton configuration while PO₄ cluster variables are characteristic of four protons configuration. Four protons state variables in eq.(A.1) the left hand side are expressed in terms of only bond state variables in the right hand side. Let a temperature T and an external field E with energy parameters $\varepsilon_0, \varepsilon_1, \varepsilon_2$ and λ be given. Further, we note that the arbitrary given values of polarization P and P' are equivalent to giving the values of bond state variables through eq.(A.5). When the bond state variables are substituted into the right hand side of eq.(A.1), the values of four proton state variables are naturally calculated. On the contrary, the geometrical relations under the uniform electric field

$$\begin{aligned}
 p_1 &= q_2 = c_0 + c_2 + a_0 + a_+ + 3d_+ + d_-, \\
 p_2 &= q_1 = c_0 + c_2 + a_0 + a_- + d_+ + 3d_-, \\
 p_3 &= q_4 = c_0 + c_2 + a_0 + a'_+ + 3d'_+ + d'_-, \\
 p_4 &= q_3 = c_0 + c_2 + a_0 + a'_- + d'_+ + 3d'_-, \\
 2r_1 &= 2s_3 = 2r_2 = 2s_4 \\
 &= 2c_0 + 2c_2 + 2a_0 + a_+ + a'_+ + 3(d_+ + d'_+) + (d_- + d'_-), \\
 2r_3 &= 2s_1 = 2r_4 = 2s_2 \\
 &= 2c_0 + 2c_2 + 2a_0 + a_- + a'_- + (d_+ + d'_+) + 3(d_- + d'_-)
 \end{aligned} \tag{B.1}$$

give values of bond variables. Thus, these bond variables again determine polarizations P and P' . Accordingly, this cycle can be repeated until the convergence within some accuracy is reached. Actually it is rigorously proved that as the iteration proceeds, the free energy is always decreased toward a local minimum which is not always the global minimum of the free energy. This property can be fully utilized in problems of hysteresis phenomena.

-
- [1] M. J. Harris, S. T. Bramwell, D. F. McMorrow, T. Zeiske, and K. W. Godfey, Phys. Rev. Lett. **79**, 2554 (1997);
M. J. Harris, S. T. Bramwell, P. C. W. Holdsworth, and J. D. M. Champion, Phys. Rev. Lett. **81**, 4496 (1998).
 - [2] T. Nagamiya: Prog. Theor. Phys. **7** (1952) 275.
 - [3] J. C. Slater: J. Chem. Phys. **9** (1941) 16.
 - [4] Y. Ishibashi, S. Ohya and Y. Takagi: J. Phys. Soc. Jpn.**33** (1972) 1545.
 - [5] Y. Ishibashi: J. Phys. Soc. Jpn.**56** (1987) 2455.
 - [6] Y. Takagi: J. Phys. Soc. Jpn. **3** (1948) 271.
 - [7] R. Kikuchi: Phys. Rev.**81** (1951) 988.
 - [8] R. Kikuchi: J. Chem. Phys.**60** (1974) 1071.
 - [9] K. Wada and Y. Ogawa: J. Phys. Soc. Jpn. **67** (1998) 112.

- [10] Eisner, I. Ya: *Izv. Akad. Nauk SSSR, Ser. Fiz.* **24** (1960) 1326 ;
Bull. Acad. Sci. USSR, Phys. Ser (English Transl.) **24** (1960) 1327.
- [11] R. Kikuchi: *Prog. Theor. Phys. Suppl.* **35** (1966) 1.
- [12] K. Wada, S. Yoshida, and N. Ihara: to be published in *J. Phys. Soc. Jpn.*

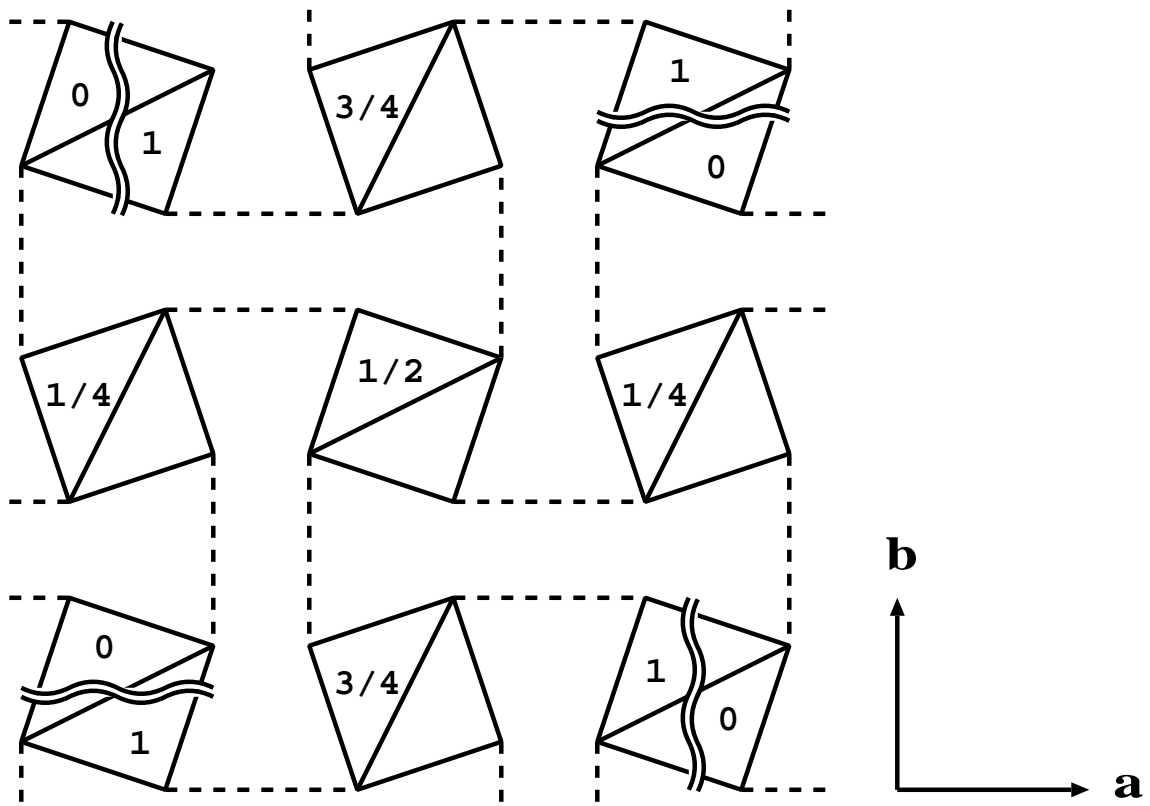
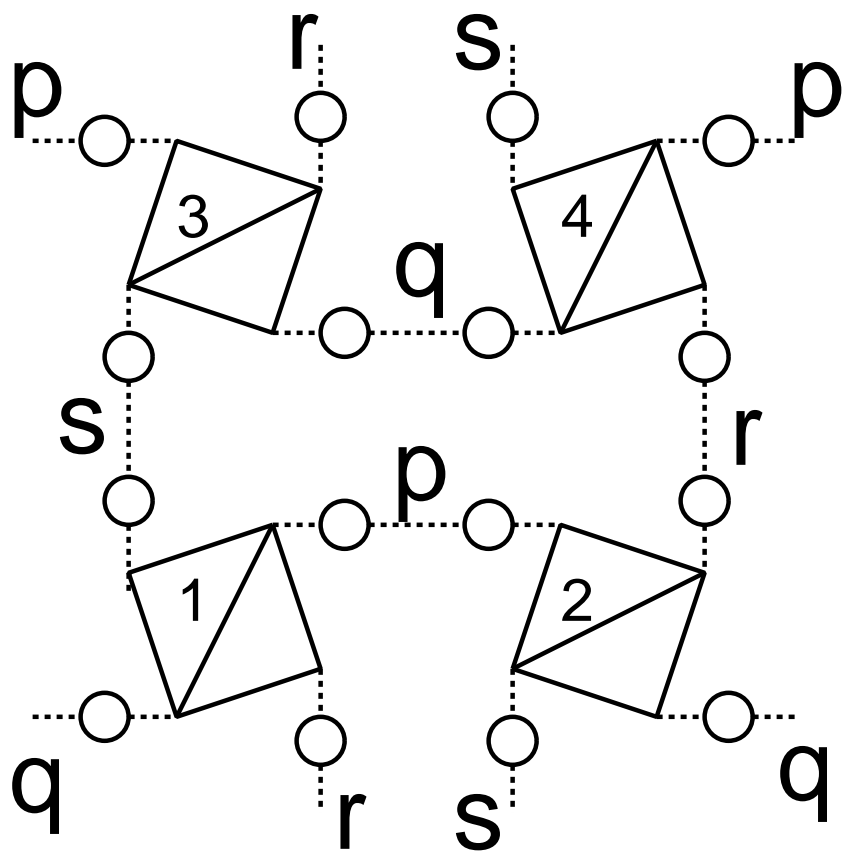


Fig. 1. The projection of atomic arrangement of ADP-type crystal on (001) plane. The number described in a PO₄ tetrahedron represents the relative height of a PO₄ tetrahedron.



 : PO₄ tetrahedron

 : H⁺ stable point

Fig. 2. Four sublattices and hydrogen bonds connecting them. Two open circles on a hydrogen bond represent two stable points of a proton.

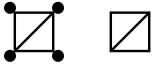
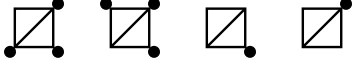
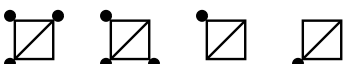
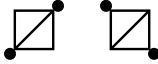
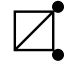
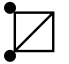
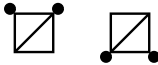
Proton Configuration	Energy	Dipole-moment along a -axis	Occurrence Probability
	ε_2	0	$c_2^{(i)}$
<hr/>			
	ε_1	$+\mu_a/2$	$d_+^{(i)}$
		$-\mu_a/2$	$d_-^{(i)}$
<hr/>			
	ε_0	0	$c_0^{(i)}$
<hr/>			
		$+\mu_a$	$a_+^{(i)}$
	0	$-\mu_a$	$a_-^{(i)}$
			$a_0^{(i)}$



Fig. 3. Energy, allotted dipole moment, and occurrence probability of proton configuration around PO_4 tetrahedron belonging to i -th sublattice.

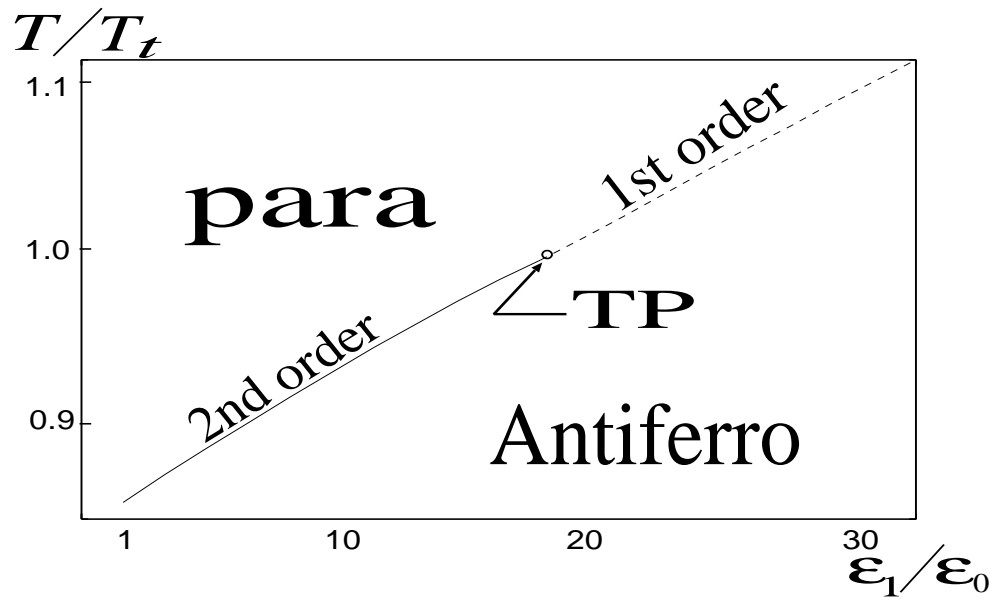


Fig. 4. The phase diagram in $\epsilon_1 - T$ space with $\epsilon_0 = 6k_B$, $\epsilon_2 = 1000k_B$, $\lambda = 232k_B$. The dotted line and solid line represents the first order and the second order phase transition temperature, respectively, and the boundary circle represents the tricritical point(TP).

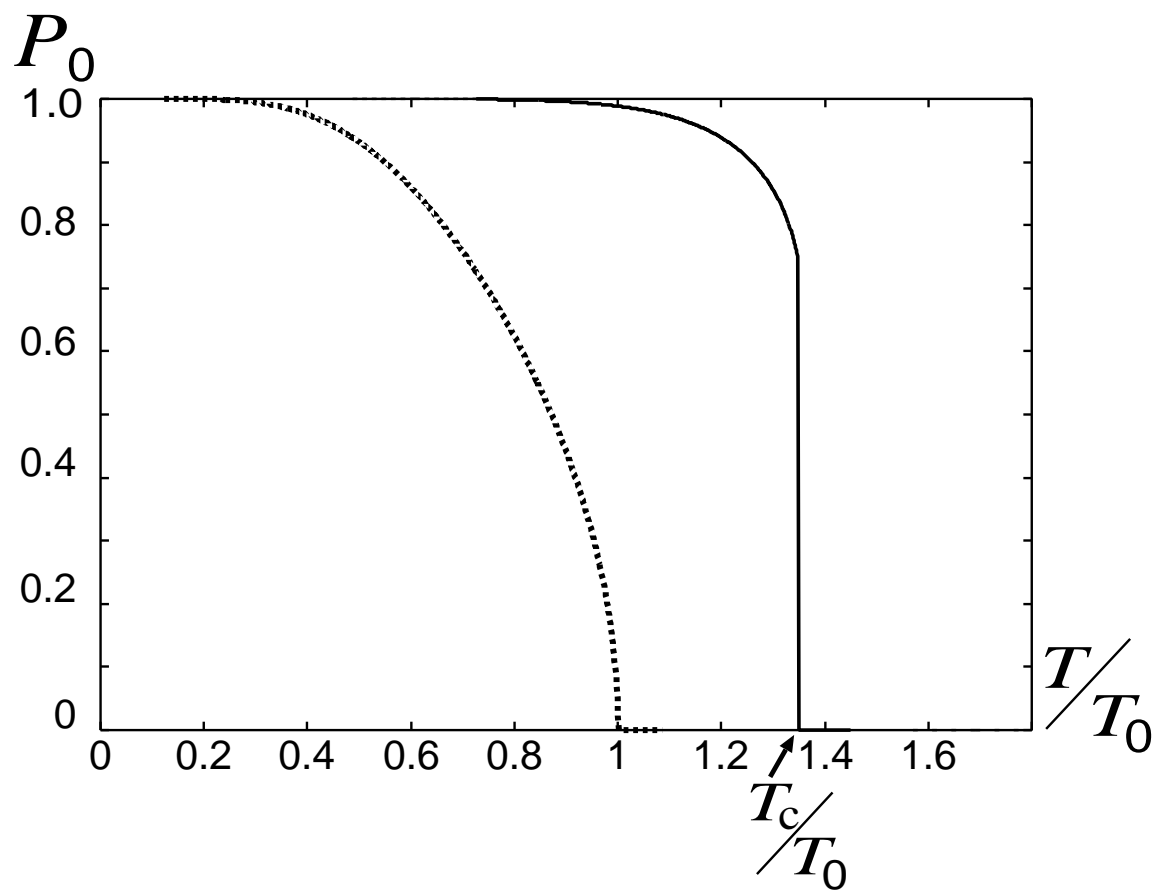


Fig. 5. The temperature dependence of antiferroelectric spontaneous polarization P_0 . The dotted line ($\varepsilon_1 = 10k_B$:second order) and the solid line ($\varepsilon_1 = 200k_B$:first order) are shown.

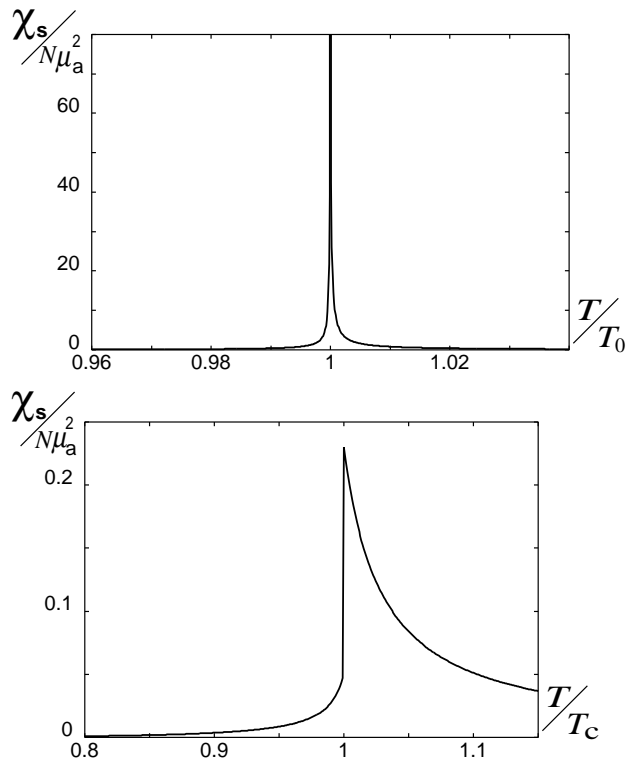


Fig. 6. The temperature dependence of staggered susceptibility χ_s . The left figure is for the second order case of $\varepsilon_1 = 10k_B$ and the right one for the first order case of $\varepsilon_1 = 200k_B$.

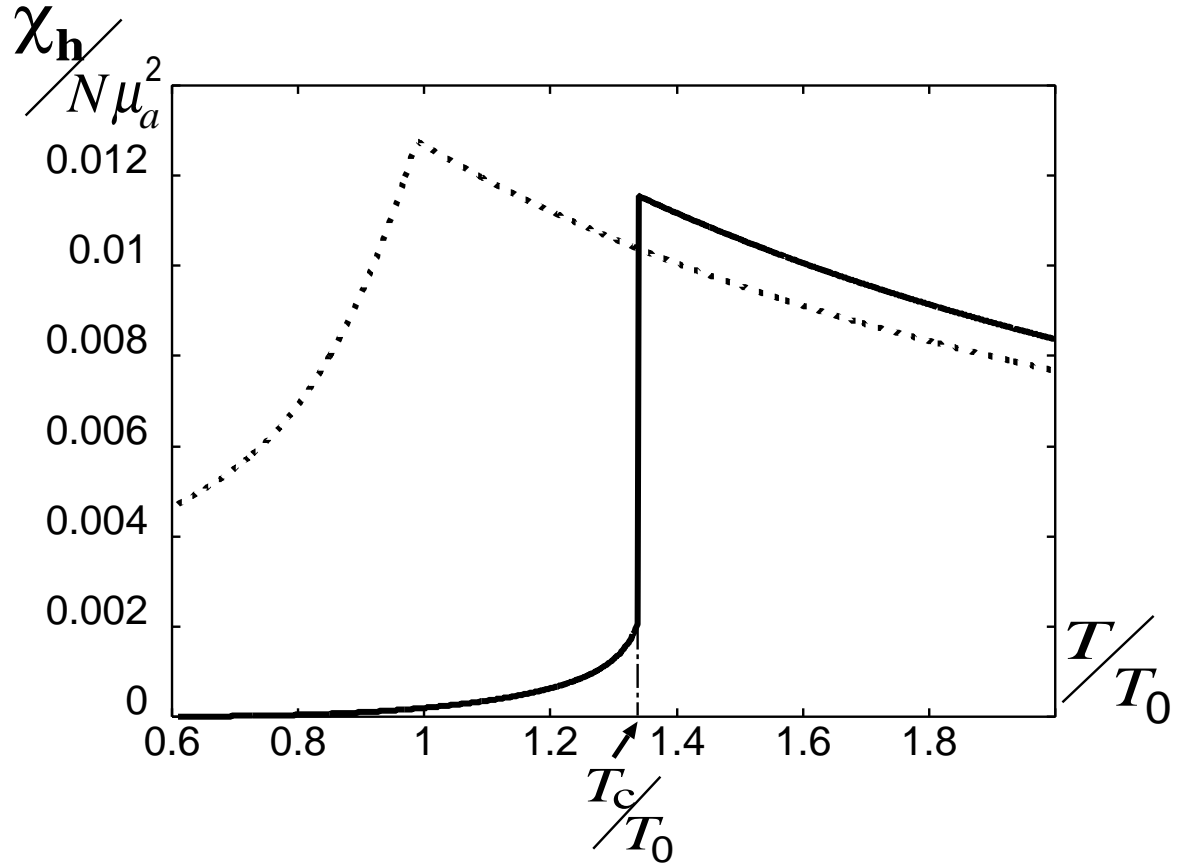


Fig. 7. The temperature dependence of uniform susceptibility χ_h . The dotted line ($\epsilon_1 = 10k_B$:second order) and the solid line ($\epsilon_1 = 200k_B$:first order) are shown.

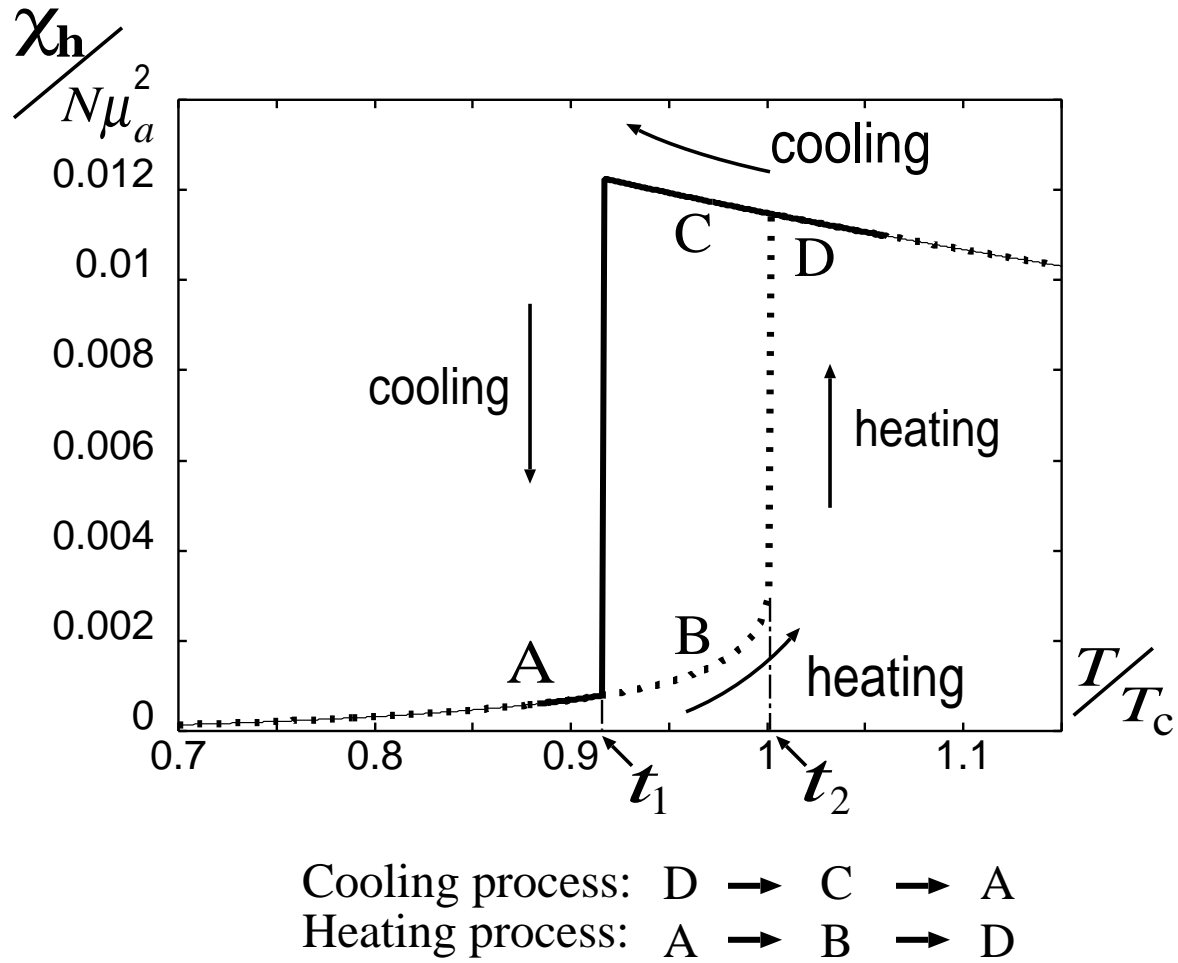


Fig. 8. Hysteresis phenomena of uniform susceptibility χ_h versus temperature T in the case of $\varepsilon_1 = 200k_B$. The solid line corresponds to cooling process and the dotted line corresponds to heating process with $T_1 = 0.9161T_c, T_2 = 1.0018T_c$.

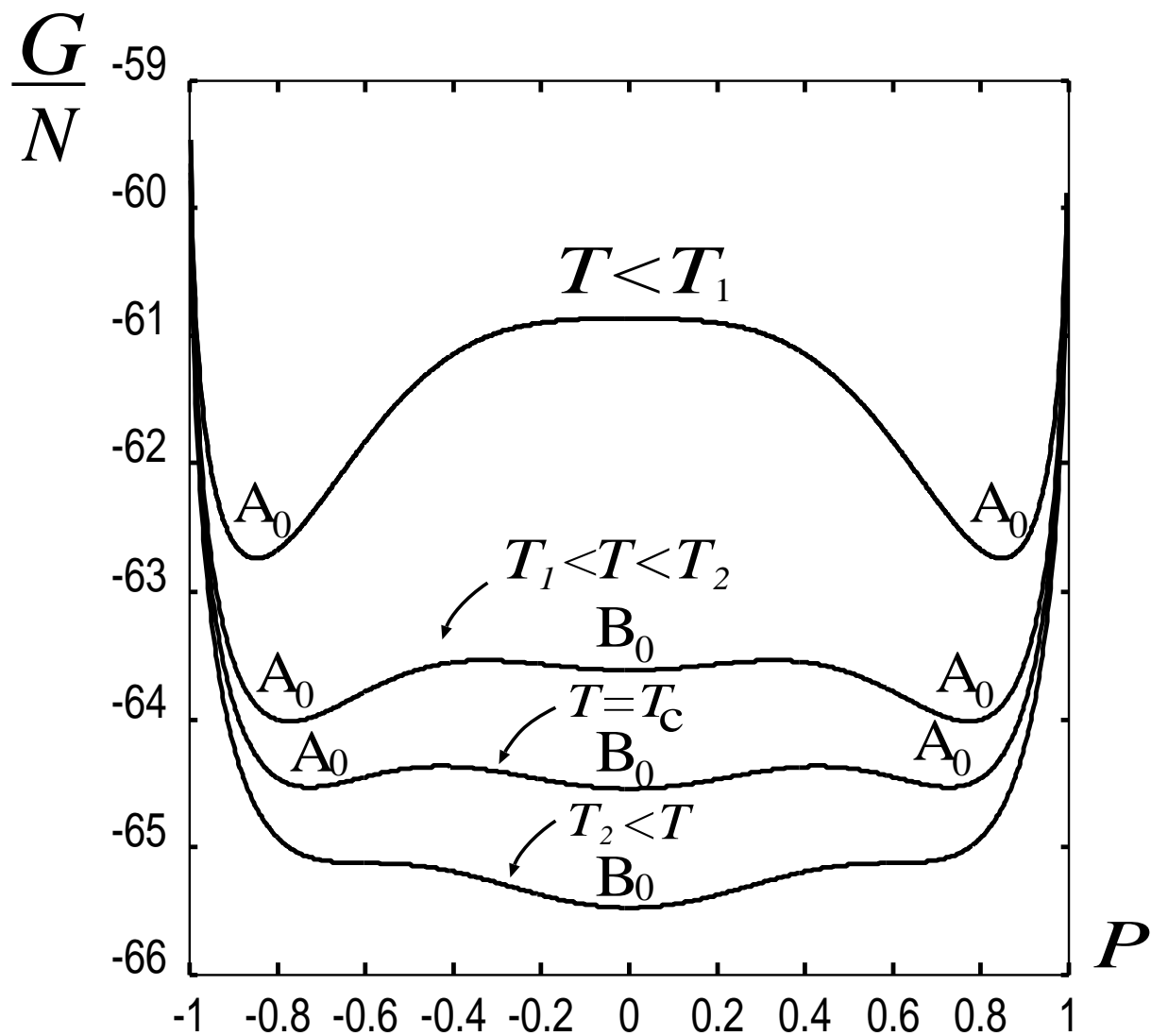


Fig. 9. Free energy profile. When $T < T_1$ there are two minima at A_0 , $T_1 < T < T_2$ three minima at A_0, B_0 , $T_2 < T$ one minimum at B_0 with $\varepsilon_1 = 200k_B$.

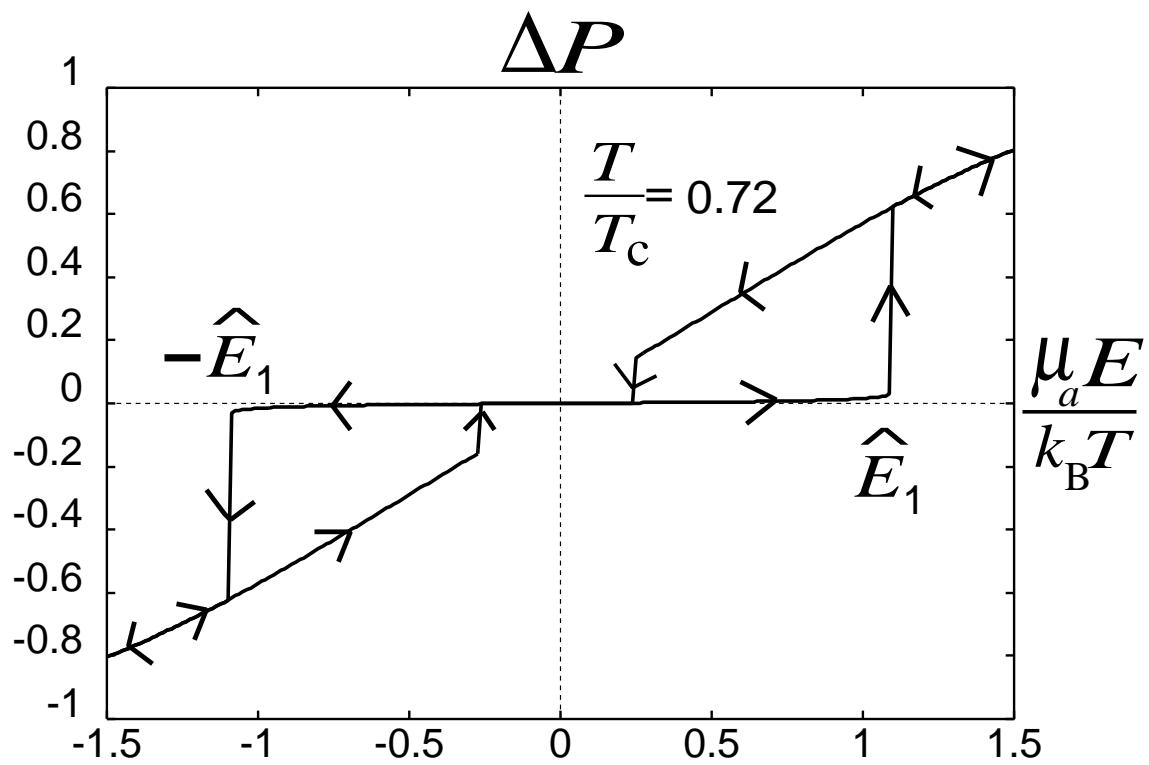


Fig. 10. Net polarization ΔP versus uniform electric field E with $\varepsilon_1 = 200k_B$.